Analysis of the Effect of Grooving the Flow Passage on the Flow Characteristics of the Fluid Passing Through the Cylindrical with a Rotating Cylinder

Meysam Hassani[1], Mahmood Ebrahimi[1*], Masoud Rahmani[2], Amin Moslemi Petrudi[2]

[1] Department of Mechanical Engineering, Iran University of Science and Technology, Tehran, P. O. B. 13114-16846, Iran
[2] Department of Mechanical Engineering, Imam Hussein University, Tehran, P. O. B. 16987-15461, Iran
[*] Corresponding author, e-mail: ebrahimi@iust.ac.ir

Abstract

Screw compressors belong to the group of positive displacement machines, which are widely used in various industries due to the advantages of these compressors compared to other industrial compressors. The distance between the moving and fixed parts of the rotating equipment is inevitable. This distance causes current leakage in all types of compressors, which reduces the efficiency of the compressor. In this research, the effect of grooving the flow passage on the flow characteristics of the passing fluid has been investigated using ANSYS CFX software. The simulation quality of positive displacement machines strongly depends on the correct prediction of the leakage current between the existing switches. It seems that creating a groove in the path of the passing current increases the thickness of the boundary layer, which acts as a barrier against the return leakage current between the rotor and the stator in the compressor. In this paper, a simplified model of the problem, which is a grooved cylinder in which a piston rotates, is investigated. First, the flow of fluid from a cylinder whose inner surface is smooth is examined, and then in boundary conditions and similar geometric dimensions, the effect of different types of grooves with different geometries on the flow characteristics will be studied. The variable is the change in drag force on the inner surfaces of the cylinder. The results show that in the best case, ie a cylinder with a single helical groove, the drag force compared to smooth geometry is 1.79 times and the flow rate is reduced by 13.21%. It is expected that the results of this study can be generalized to reduce leakage current between the rotor and the screw compressor housing.

Keywords: Grooved cylinder, Screw compressor, Drag force, ANSYS CFX.

1 Introduction

Screw compressors are among the positive displacement compressors of rotational type and are one of the most common gas compressors used in various industries. A positive displacement compressor is a machine that transports gas from a low-pressure to a high-pressure section by trapping it in a chamber and then reducing its volume, which reduces the pressure in the gas. In addition to gas, these types of compressors are also capable of condensing steam and refrigerants. Screw compressors supply compressed gas in various industries such as construction, industry, food, chemical processes, pharmaceuticals, and metallurgy. These compressors are also used in the refrigeration and refrigeration, air conditioning, and supercharging industries. It is necessary to consider the distance between the rotor and the stator in the screw compressor, but this air gap causes the fluid flow to leak from the high-pressure part to the low-pressure part. Which in turn has negative effects on compressor performance, including volume efficiency. Leakage between the rotor tip and the compressor housing is one of the most important leaks that occur in this compressor. The tip leakage current causes flow instabilities, clogging, and

ultimately reduced turbomachine efficiency. Nowadays, the desire of designers for compressors with lower weight and wider operating range is a growing vision. Therefore, controlling tip leakage current is essential due to its importance in initiating rotational instabilities, and much research has been done to develop methods for controlling tip leakage current. Shell deformation is known as an efficient and effective method to increase the efficiency and stability of axial compressors. So far, different shell shapes have been designed and tested to increase the compressor operating range. Among the various shell modification methods that have been studied so far, we can mention the circumferential groove [1], slot [2], and stepped tip gap [3]. Many researchers have studied various shell modification methods in axial and centrifugal compressors, to extend the range of stable compressor performance. But most of these methods have resulted in reduced compressor efficiency. In an article, Solki et al. [4] have examined one of the new methods of shell modification to improve the performance of compressors. Step joint seam is one of the suitable methods for

modifying the compressor shell, which has recently been proven to be effective in the field of axial compressors. In their study, the effects of step tip seam on improving the stall margin of a centrifugal compressor have been evaluated numerically for the first time. The simulation was performed with the help of Fluent software and using the k-ϵ turbulence model. To find the optimal geometry of the step tip seam, seven different shell geometries along with a smooth shell compressor have been considered. Examination of velocity counters and flow line patterns on planes perpendicular to the flow direction shows that by creating a shell with a stepped tip seam, the blade tip leakage current is weakened and the amount of flow obstruction in the main compressor passage is reduced. Therefore, the step of the stepped tip increases the range of stable compressor performance and delays the occurrence of the stall phenomenon. Shabbir et al. [5] used reliable numerical analysis to understand the mechanism of stall margin improvement. They applied this analysis to an axial compressor rotor affected by the shell groove. This analysis showed that the rotor performance range is affected by the shell groove. Gao et al. [6] performed a three-dimensional numerical analysis on NASA's low-speed centrifugal compressor, with peripheral grooves as well as a simultaneous air intake. They analyzed the flow structure at the blade tips and showed that this type of shell modification could extend the range of the compressor's stable operating range by about 20% without a drop in inefficiency. Legras et al. [7] investigated The effects of peripheral grooves on NASA 37 sound transduction rotors were performed to improve the blade tip leakage current near the surge conditions by examining their reliable calculations using Elsa software using the finite volume method. They showed that the grooves limit the development of the vane tip leakage direction perpendicular to the blade chord by reducing the momentum present in its rotational mechanism. Peng et al. [8] investigated three different shell modification methods, including peripheral grooves, air suction with circumferential grooves, recess vane in a high-speed centrifugal compressor. In this research, numerical modeling of flow was performed using a three-dimensional model. They proved that this type of shell modification can increase the range of stable compressor performance, but reduce the compressor efficiency. Peng et al. [9] analyzed eight different shapes of peripheral grooves numerically. They used the Euranus solver of NUMECA FINE software suite to solve Reynolds's median three-dimensional equations with the Spalart-Allmaras turbulence model. He found that proper selection of groove parameters plays an important role in improving

compressor stability. Zheng et al [10] Stability improvement of high-pressure-ratio turbocharger centrifugal compressor by asymmetrical flow control. He examined four different types of shell correction, including circumferential groove, shell protrudes, the combination of circumferential grooves and shell protrusion, and radial grooves within the gap between the impeller and the diffuser. The results of this study showed that this type of shell modification improves the range of stable compressor performance. Wilke et al. [11] presented the effects of two peripheral groove mechanisms and a specific type of slot on the flow field of a single row of high-pressure compressor blades, using the solution of Reynolds averaged three-dimensional equations. Rabe et al. [12] also investigated the effects of using three peripheral grooves with different aspect ratios in an axial compressor on improving the stall margin. They experimentally and numerically proved that these grooves improve the stall margin by reducing the angle of incidence of the flow and subsequently improving the flow field, and found that shallow grooves have a better effect on improving the stall margin. The effects of stepper tip seam and change of blade tip to shell seam rate on the performance of an axial acoustic compressor were investigated experimentally by Donald et al. [13]. They examined nine different shell geometries, including three types of stepper-tip seams, which were applied to three types of shells with different fin-to-shell seam seams. Their goal was to find the optimal state of this combination of geometries. How to choose the optimal mode depends on the compressor design goals, based on the highest pressure-to-efficiency ratio or the widest range of compressor stable performance. They found that at small and medium tip joint sizes, the shell groove improved efficiency and increased the pressure ratio over a wide range of operating conditions. Hong et al. [14] also numerically studied the effect of grooves in the pipe on the flow characteristics. Their results show that increasing the height of the groove increases the coefficient of friction and causes vortices in the grooves and outside them. They also found that the coefficient of friction depended on the number of grooves. Most studies on the effect of shell deformation have been performed in a laboratory manner and are limited to the study of the general characteristics of the compressor. Little research has been found to accurately study the dynamics of leakage flow interaction with the shell. Over the past decade, several studies have focused on the development of numerical analysis to investigate the dynamics of tip leakage flow in interaction with the shell. As mentioned in the introduction, it seems that shell modification in axial and centrifugal

compressors has been studied and no research has been done on the creation of grooves in the shell and their effect on the performance of screw machines.

2 Governing Equations

For a Newtonian fluid in three-dimensional motion, the relationship of the flow field to the velocity vector is:

$$\vec{v} = \vec{e}_x u + \vec{e}_y v + \vec{e}_z w \tag{1}$$

Where u, v and w, are three velocity vector components in the Cartesian coordinate system with unit vectors $\vec{e}_x$ ، $\vec{e}_y$ and $\vec{e}_z$ are also determined by pressure P and temperature T. To determine these five variables, five equations are as follows:

• Continuity equation (conservation of mass)

In incompressible fluids, the material derivative of density over time will be zero:

$$D\rho/Dt = 0 \tag{2}$$

as result:

$$div\vec{v} = 0 \tag{3}$$

• Motion size equation (conservation of momentum)

To calculate the velocity of the fluid flow field, linear and angular momentum equations will be needed. These equations are generally derived from Newton's second law and are widely used in the Navier-Stokes equations and computational fluid dynamics.

The final form of these equations is shown in three directions x, y, and z, respectively:

$$\rho\left(\frac{\partial u}{\partial t} + u\frac{\partial u}{\partial x} + v\frac{\partial u}{\partial y} + w\frac{\partial u}{\partial z}\right)$$
$$= -\frac{\partial P}{\partial x} + \rho g_x + \mu\left(\frac{\partial^2 u}{\partial x^2} + \frac{\partial^2 u}{\partial y^2} + \frac{\partial^2 u}{\partial z^2}\right)$$
$$\rho\left(\frac{\partial v}{\partial t} + u\frac{\partial v}{\partial x} + v\frac{\partial u}{\partial y} + w\frac{\partial v}{\partial z}\right)$$
$$= -\frac{\partial P}{\partial y} + \rho g_y + \mu\left(\frac{\partial^2 v}{\partial x^2} + \frac{\partial^2 v}{\partial y^2} + \frac{\partial^2 v}{\partial z^2}\right) \tag{4}$$
$$\rho\left(\frac{\partial w}{\partial t} + u\frac{\partial w}{\partial x} + v\frac{\partial w}{\partial y} + w\frac{\partial w}{\partial z}\right)$$
$$= -\frac{\partial P}{\partial z} + \rho g_z + \mu\left(\frac{\partial^2 w}{\partial x^2} + \frac{\partial^2 w}{\partial y^2} + \frac{\partial^2 w}{\partial z^2}\right)$$

• Energy equation

$$\frac{\partial}{\partial t}\left[\rho\left(e + \frac{V^2}{2}\right)\right] + \vec{V}\cdot\left[\rho\left(e + \frac{V^2}{2}\right)\vec{V}\right]$$
$$= \rho\dot{q} - \nabla\cdot(P\vec{V}) + \rho(\vec{f}\cdot\vec{V}) + \dot{Q}'_{Viscosity} \tag{5}$$
$$+ \dot{W}'_{Viscosity}$$

Where $\rho\dot{q}$ thermal spring, $\nabla\cdot(P\vec{V})$ pressure force work, $\rho(\vec{f}\cdot\vec{V})$ volumetric force work, $\dot{Q}'$ viscous and $\dot{W}'$ viscous represent the appropriate forms of vicious sentences.

• Turbulence dissipation equation

$$\rho u_i \frac{\partial\varepsilon}{\partial x_i} = C_{\varepsilon 1}\frac{\varepsilon}{k}\sigma_{ij}\frac{\partial u_j}{\partial x_i} - C_{\varepsilon 2}\rho\frac{\varepsilon^2}{k}$$
$$+ \frac{\partial}{\partial x_i}\left[\left(\mu + \frac{\mu_t}{\sigma_k}\right)\frac{\partial\varepsilon}{\partial x_i}\right] \tag{6}$$

• Turbulence viscosity equation

$$\mu_t = \rho C_\mu \frac{k^2}{\varepsilon} \tag{7}$$

where r is the fluid density, m is the dynamic viscosity, ui is components of the velocity vector, k is turbulence kinetic energy, ε is turbulence dissipation rate, and σ_{ij} is the Reynolds stress tensor.

3 Problem statement

First, the smooth cylinder containing the flow is examined, then three different geometries are considered to study the effect of the groove, in one geometry the grooves are rings perpendicular to the flow and two geometries are with the helical groove. The geometries were created using Katia software. The dimensions of the inner surface of the cylinder are as follows. The diameter is 72 mm and its height is 72 * 1.406 = 101.232 mm, which is similar to the usual size of the screw compressor shell. The thickness of the cylindrical shell is 2 mm. The cross-section of all grooves in this section is the same as before. The groove is selected with a rectangular cross-section with a length of 3 mm and a depth of 1 mm. The grooves are created in three different models. In one of the geometries, several grooves are created as a complete loop, the angle between the grooves and the direction of flow is perpendicular and the distance between the grooves is 17 mm.
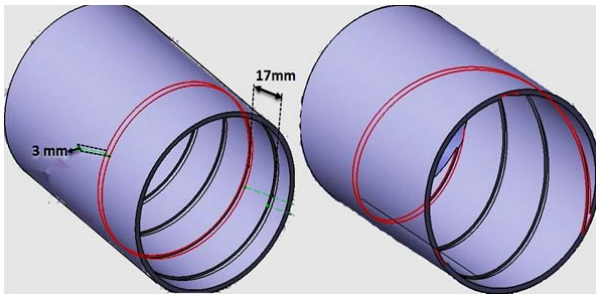
Fig. 1 Grooved cylinder, grooves in a ring and a spiral with a complete rotation.

The next geometry is that three grooves are created on the inner circumference of the cylinder with an angle difference of 120 degrees relative to each other at the beginning of the geometry and they advance in a helical manner on the inner surface of the cylinder and reach the end of the cylinder by turning in a semicircle. The shape of the next geometry is similar to the previous one, except that the grooves are rotated a complete circle from the beginning to the end of the cylinder, ie in this case the position of the groove is the same at the beginning and end of the cylinder. Can be seen in Fig 1.

• **Meshing**

The computational area is networked with a disorganized mesh. After examining the issue of network independence, the fluid region has meshed with 1393514 elements. 574533 is the element related to the boundary layer mesh. The height of the first node from the wall is 14.8e-6 m. The mesh can be seen in Fig 2.

Fig. 2 Disorganized mesh - the area inside the smooth cylinder.

To save time and memory, the solid region of the cylindrical shell has been removed from the calculations. Note that since the problem of heat transfer between the fluid and solid regions is not considered, the elimination of the solid region will not affect the results such as velocity and point pressure, or even if we needed to solve the energy equation in the solution domain Adiabatic process

for the surface of the cylinder, do not enter the solid area in the calculations without special concern.

• **Apply boundary conditions and adjust the solver**

The velocity at the inlet is 40 m / s and the absolute pressure at the outlet of the cylinders is set to 1 atm. Considering the velocity, the current is considered incompressible. The parameter under consideration is the drag force on the cylindrical wall, so the flow is of the viscous type. The non-slip condition is set on the inner surfaces of the cylinders. The velocity contours, which will be presented from the side view in the next section, correspond to the points on the XY plane as shown in Fig 3. The SST turbulence model is used to calculate and simulate the flow.
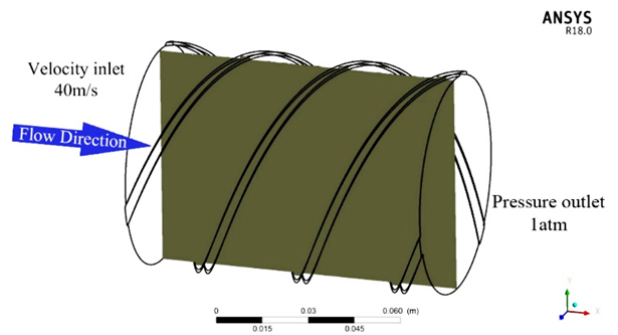
Fig. 3 Internal surface of the cylinder, prevailing boundary conditions.

• **Validation**

To check the accuracy of the results, the mode of using circular grooves has been compared with the reference [14]. Figure 4 shows the parameters used in this section.
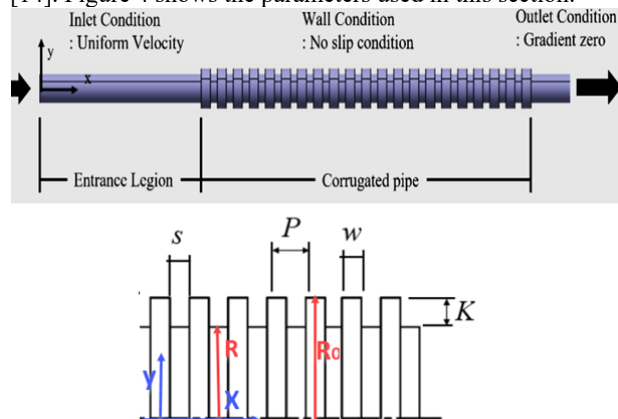
**Fig. 4** Validation geometric parameters [14].

The problem is that the current from the left enters a tube with 21 grooves according to the shape, the flow velocity is compared. In the comparison, the corrugated pipe has 21

grooves, the geometric characteristics of the pipe are presented in Table 1 according to the figure.

Table 1 Geometric parameters invalidation.

| D (mm)	S (mm)	P (mm)	w (mm)	K (mm)	w/K	P/K
25.9	4.403	5.5685	1.1655	2.331	0.5	2.389

The velocity vector near the pipe wall, y / R = 0.98, is compared with the reference in the second, fifth, and tenth loops of the pipe section after the loops. Fig. 5 compares the velocity vectors with the reference and shows that the simulation results are accurate enough. It is also seen in this figure that after each groove the velocity decreases first and then gradually increases until the next groove starts.
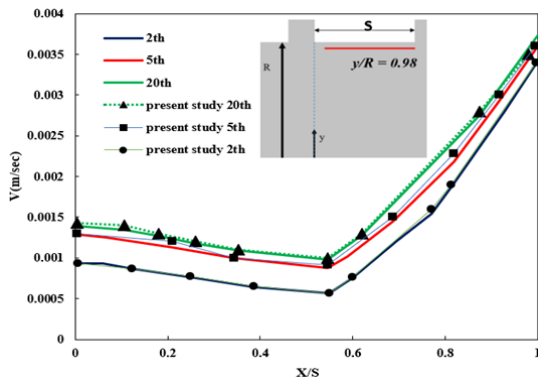
**Fig. 5** Comparison of velocity size near the pipe wall [14].

4 Results and discussion

In Fig. 6, the velocity contour of the four geometries is shown simultaneously for easier comparison of the thickness of the boundary layer. Note that the shape of the velocity contours corresponds to the upper half of the geometry. Carefully in the boundary layer, we notice the changes caused by the groove. The thickness of the boundary layer increases cross-sectionally as the current passes through the groove.
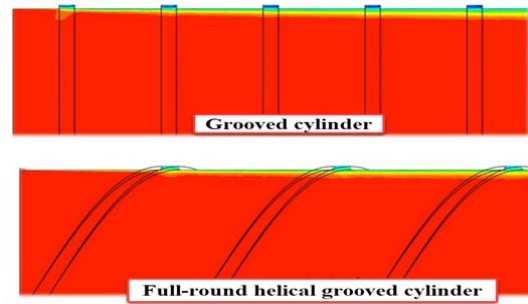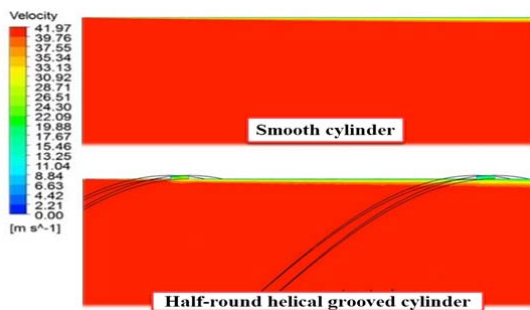
Fig. 6 Speed contour in four different geometries.

According to Fig. 6, in all grooved geometries, the thickness of the boundary layer has increased relative to the smooth state. In helical groove geometry, the thickness of the boundary layer increases with increasing during the groove period from half-circle to one-circle. This increase may be due to the increase in the angle of the groove and its approach to the right angle concerning the direction of flow. Fig. 7 shows a diagram of the drag force on the inner surfaces of the cylinders. In all cases, we see an increase in this force compared to the flat cylinder. Here, too, the drag force in the cylinder with the circular helical groove is greater than that of the semicircular groove. The inner surfaces of the cylinder with a completely circular helical groove are applied more drag force than the other cases, and this geometry seems to be closer to our goal. The drag force in this mode is more than 2 times that of the non-groove mode.
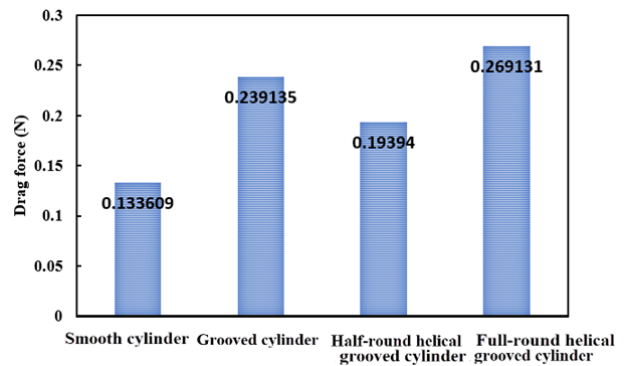
Fig. 7 Comparison of drag force on the inner surface of cylinders.

• Fluid flow through the distance between the cylinder and the rotating piston

This section is very similar to the previous section, and the only difference is in the rotating cylinder, which is at the center of the geometry of the previous section with a rotating angular velocity, and the fluid is passing through

the space created between these two cylinders. The parameter under consideration is the amount of drag applied to the surfaces of the two cylinders and the flow rate in different geometries. According to the results obtained in the previous sections, it is expected that in grooved geometries the amount of drag force will increase and the amount of flow rate will decrease. The dimensions of the outer cylinder are similar to the cylinders of the previous section. That is, the diameter of the cylinder is 72 mm and its height is 100.232 mm. The inner cylinder has an equal height and a diameter of 68 mm. The axes of the cylinders are on top of each other. As a result, the distance between the cylinders is 2 mm. Fig. 8 shows the model used.
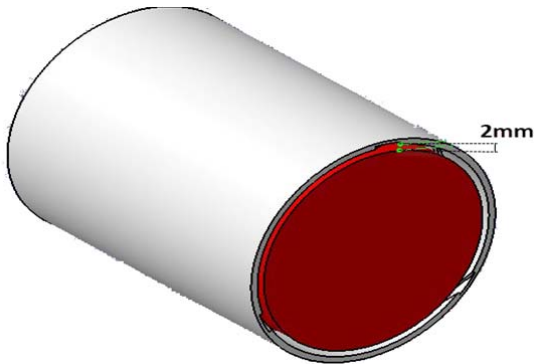

Fig. 8 Grooved cylinder with rotating piston in its center.

Due to the almost complex geometry, the unorganized mesh is used to network the solution domain. After examining the solution independent of the network, the number of elements reached 8181184, of which 5233360 is related to the boundary layer mesh. Note that in this case the boundary layer mesh is created on the two walls. According to Fig. 9, in this part, the simulation of solid parts of geometry, which include the outer cylindrical shell and the inner cylinder volume, is ignored and the computational area is focused only on the space between the two cylinders that is filled with fluid.
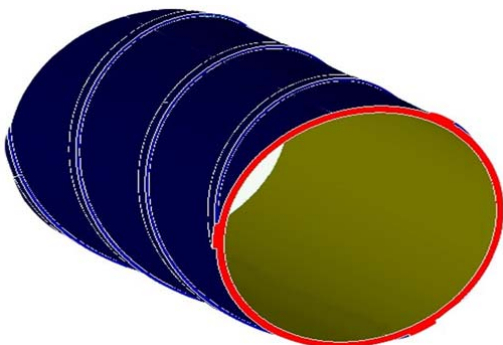

Fig. 9 Computational area, the space between two cylinders.

The height of the first floor of the border layer mesh from the wall surfaces is equal to 1.5e-6 m and with a growth coefficient of 1.4 to 10 floors, the border layer mesh is laid.

Fluid flow occurs due to the pressure difference between the inlet and outlet. The value of this pressure difference is equal to 10132.5 Pa. The maximum velocity obtained from the initial solution under these conditions was about 100 m / s. As a result, the type of flow is considered incompressible, viscous, and permanent. The condition of non-slip is applied on the walls. In two cases where the outer cylinder is flat or has a ring groove, it does not matter which direction the piston rotates due to the symmetry of the geometry. But in the other two cases, the helical groove, this direction of rotation is important. First, a position is considered that is opposite to the direction of rotation of the piston and groove, ie one clockwise and the other counterclockwise, and then the agreeable position and the difference between the two will be compared. In this section, the SST turbulence model is used to calculate and simulate the flow. The two-dimensional extraction results are for points on the XY plane that are in the solution domain. Fig. 10 shows the velocity contour of one of the geometries. It can be seen that the fluid flow fluctuates rapidly as it passes through the grooves.
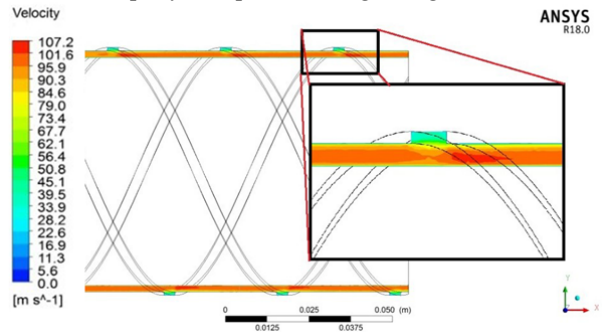

Fig. 10 Speed contour (cylinder with a single helical groove).

For a better comparison, all velocity counters are brought together in one shape. In Fig. 11, concerning the contours, the flow velocity in all grooved states is reduced relative to the smooth geometry. And only temporarily did the fluid velocity near the grooves increase.
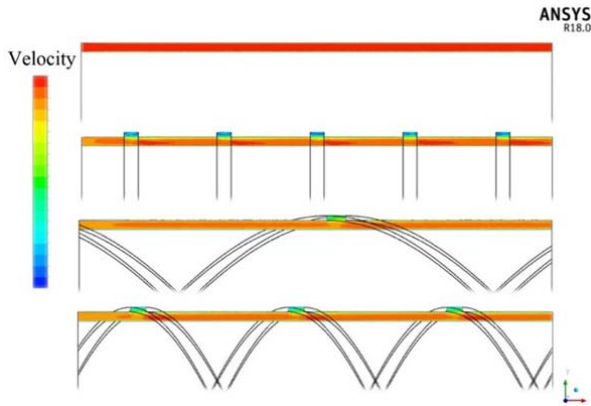
Fig. 11 Speed contour for all geometries.

The following are quantitative results in Table 2, which include information such as drag force on the walls, fluid flow rate. And diagrams are extracted accordingly for clearer examination. The last two rows of the table correspond to the position that agrees with the direction of rotation of the groove and the piston. In all grooved cases, the drag force is increased and the flow rate is reduced compared to the smooth state. According to the diagram in Fig. 12, the more the total drag force on the current-carrying surfaces increases, the more the flow rate decreases. By simple mathematical calculation, it can be seen that in the best case, that is, a cylinder with a single helical groove, the drag force is 1.79 times greater than that of smooth geometry, and the flow rate is reduced by 13.21%.

Table 2 Quantitative information extracted.

| Type of geometry	Flow rate kg / s	Total drag force (N)	Drag force on piston (N)	Drag force on the shell (N)
smooth	0.0512474	1.783553	0.848263	0.93529
Ring groove	0.0449852	3.120504	0.766782	1.58694
Half-round spiral groove	0.0468589	2.835732	0.830932	1.20573
Single round spiral groove	0.0444817	3.186923	0.79907	1.55771
Half-round groove agrees	0.0468852	2.862216	0.830143	1.20193
A single round groove agrees	0.0445084	2.352307	0.797957	1.55435
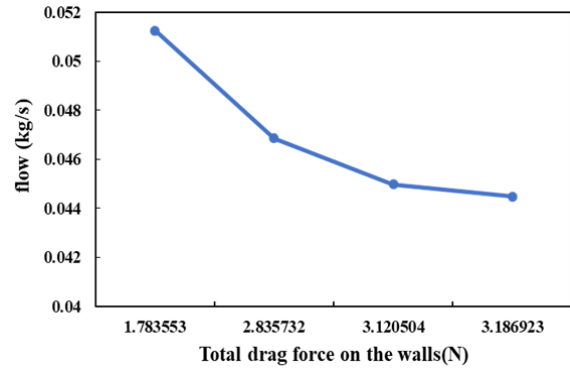
Fig. 12 Increasing the drag force on the passage walls and decreasing the flow rate.

5 Conclusion

In the study of preventing backflow in screw compressors, in this research, a simplified model investigates the problem of screw compressor, which is a grooved cylinder in which a piston rotates. First, the flow of fluid from a cylinder whose inner surface is smooth is examined, and then in boundary conditions and similar geometric dimensions, the effect of different types of grooves with different geometries on the flow characteristics will be studied. The desired change is the change in drag force on the inner surfaces of the cylinder. The results show that in the best case, ie a cylinder with a single helical groove, the drag force compared to smooth geometry is 1.79 times and the flow rate is reduced by 13.21%. It is expected that the results of this study can be generalized in reducing the leakage current between the rotor and the screw compressor housing and can increase the efficiency of such rotary machines with this technique.

Acknowledgment

References

[1] Zhang, H. G., W. L. Chu, and Y. H. Wu. "Numerical investigation of the circumferential grooved casing treatment as well as analyzing the mechanism of improving stall margin." In New Trends in Fluid Mechanics Research, pp. 448-451, 2007. https://doi.org/10.1007/978-3-540-75995-9_145

[2] Yu, Q. L., and Ling. L. "The experimental researches on improving operating stability of a single-stage transonic fan." In ASME Turbo Expo 2002: Power for Land, Sea, and Air, pp. 1133-1139, 2002. https://doi.org/10.1115/GT2002-30640

[3] Taghavi, R., and Eslami. S. "Effects of casing treatment on behavior of tip leakage flow in an isolated axial compressor rotor

blade row." Journal of the Chinese Institute of Engineers 36, no7: 819-830, 2013.
https://doi.org/10.1080/02533839.2012.747058

[4] *Solki, E., and Afshari. H. "Computational analysis of stepped tip gap casing effect on the performance of a centrifugal compressor." Modares Mechanical Engineering 14, no.3: 136-144, 2014.*
https://mme.modares.ac.ir/article-15-11317-en.html

[5] *Shabbir, A., and Adamczyk. J. "Flow mechanism for stall margin improvement due to circumferential casing grooves on axial compressors." Journal of Turbomachinery, 127(4): 708-717, 2005.*
https://doi.org/10.1115/1.2008970

[6] *Gao, P., W. L. Chu, and Y. H. Wu. "The mechanism of stall margin improvement in a centrifugal compressor with the air bleeding circumferential grooves casing treatment." In New Trends in Fluid Mechanics Research, pp. 482-485, 2007.*
https://doi.org/10.1007/978-3-540-75995-9_154

[7] *Legras, G. N, and Trebinjac. I. "Numerical analysis of the tip leakage flow field in a transonic axial compressor with circumferential casing treatment." Journal of Thermal Science 19, no. 3: 198-205, 2010.*
https://doi.org/10.1007/s11630-010-0198-y

[8] *Peng, G., and Zhang. S. "Numerical investigation of the different casing treatment in a centrifugal compressor." In 2010 Asia-Pacific conference on wearable computing systems, IEEE, pp. 51-54, 2010.*
https://doi.org/10.1109/APWCS.2010.20

[9] *Peng, G., and Zhang. S. "Notice of Retraction: The analysis of tip flow field in a centrifugal compressor with different circumferential grooves casing treatment." In 2010 International Conference on Computer and Communication Technologies in Agriculture Engineering, IEEE, vol. 1, pp. 21-24, 2010.*
https://doi.org/10.1109/CCTAE.2010.5543690

[10] *Zheng, X., and Tamaki. H. "Stability improvement of high-pressure-ratio turbocharger centrifugal compressor by asymmetrical flow control—Part II: Nonaxisymmetrical self-recirculation casing treatment." Journal of turbomachinery, 135, no. 2, 2013.*
https://doi.org/10.1115/1.4006637

[11] *Wilke, I., and H-P. Kau. "A numerical investigation of the influence of casing treatments on the tip leakage flow in an HPC front stage." In Turbo Expo: Power for Land, Sea, and Air, vol. 3610, pp. 1155-1165. 2002.*
https://doi.org/10.1115/GT2002-30642

[12] *Rabe, D. C., and C. Hah. "Application of casing circumferential grooves for improved stall margin in a transonic axial compressor." In Turbo Expo: Power for Land, Sea, and Air, vol. 3610, pp. 1141-1153. 2002.*
https://doi.org/10.1115/GT2002-30641

[13] *Donald, T., Paul I., and Rabe. D. "Experimental investigation of stepped tip gap effects on the performance of a transonic axial-flow compressor rotor.477-486, 1998.*
https://doi.org/10.1115/1.2841743

[14] *Hong, K., and Hong, R. "Numerical Study on the Effect of the Pipe Groove Height and Pitch on the Flow Characteristics of Corrugated Pipe." Energies, 14, no. 9: 2614, 2021.*
https://doi.org/10.3390/en14092614